Iraqi Journal of Physics, 2018 *Vol.16, No.38, PP. 35-41*

DOI: 10.20723/ijp.16.38.35-41

Annealing effects on optical and structural properties of chromium oxide thin film deposited by PLD technique

Shahad E. Abdughani and Fuad T. Ibrahim

Department of Physics, College of Science, University of Baghdad, Baghdad, Iraq

E-mail: Fuadtariq2002@yahoo.com

Abstract

Optical properties of chromium oxide (Cr_2O_3) thin films which were prepared by pulse laser deposition method, onto glass substrates. Different laser energy (500-900) mJ were used to obtain Cr_2O_3 thin films with thickness ranging from 177.3 to 372.4 nm were measured using Tolansky method. Then films were annealed at temperature equal to 300 $^{\circ}$C. Absorption spectra were used to determine the absorption coefficient of the films, and the effects of the annealing temperature on the absorption coefficient were investigated. The absorption edge shifted to red range of wavelength, and the optical constants of Cr_2O_3 films increases as the annealing temperature increased to 300 $^{\circ}$C. X-ray diffraction (XRD) study reveals that Cr_2O_3 thin films are amorphous; while the crystal structure of annealed Cr_2O_3 films is rhombohedral after annealing at 300 $^{\circ}$C for two hour. AFM studies of Cr_2O_3 thin films exhibit a smooth and well dispersed on the surface.

Key words

Cr_2O_3, PLD technique, X-ray diffraction.

Article info.

Received: Jan. 2018
Accepted: Mar. 2018
Published: Sep. 2018

تأثير التلدين على الخصائص البصرية والتركيبية لغشاء أوكسيد الكروميوم المرسب بتقنية الترسيب بالليزر النبضي

شهد عماد الدين عبد الغني و فؤاد طارق إبراهيم

قسم الفيزياء، كلية العلوم، جامعة بغداد، بغداد، العراق

الخلاصة

تم في هذا البحث دراسة الخصائص البصرية لأغشية اوكسيد الكروميوم (Cr_2O_3) الرقيقة والتي رسبت بطريقة الترسيب بالليزر النبضي على ارضيات زجاجية باستخدام مدى طاقات يتراوح بين (500-900) ملي جول. سمك الغشاء المحضر (177.3-372.4) نانومتر. وتم تلدين الاغشية بدرجة حرارة 300 $^{\circ}$C. استخدمت اطياف الإمتصاصية لحساب معامل الامتصاص للاغشية، وتم دراسة تأثير التلدين على معامل الامتصاص، وان حافة الامتصاص تم ازاحتها بأتجاه اللون الاحمر من الطيف المرئي والثوابت البصرية تزداد بزيادة حرارة التلدين. اظهرت صورة الـ X-ray بأن غشاء Cr_2O_3 غير متبلور أما التركيب البلوري للغشاء الملدن عند 300 $^{\circ}$C فأنه يمتلك تركيب سداسي منتظم بينما بينت فحوصات AFM بان الغشاء ذو سطح صقيل.

Introduction

Chromium oxide (Cr_2O_3) nanoparticles are of interest for applications such as green pigments, wear resistance، thermal protection, digital recording systems, and chemical catalysts [1]. Cr_2O_3 nanoparticles have been prepared and characterized by many different researchers [2], and the resulting particle size depending on the method of preparation.

Chromium oxides (Cr_2O_3) are important technological materials because of their intrinsic properties, such as high temperature stability. In particular, among the many chromium oxides, Cr_2O_3 is the most

thermodynamically stable phase above 500 °C, and is particularly interesting for its very high hardness and chemical resistance properties. It is used as a protective coating on high-temperature battery electrodes, as intermediate layers in corrosion-resistant applications on semi-conductors and metals, as wear-resistant layers on magnetic particles, and as anti-oxidation layers on metals such as stainless steel [3, 4]. Liquid crystal displays used low- reflective Cr_2O_3/Cr films were used as black matrix films [5]. Literature reports indicate that Cr_2O_3 thin films have been produced by a number of techniques by a number of researchers. These include the vacuum evaporation [6], sputtering [4], Chemical Vapor Deposition (CVD) [5], Spray pyrolysis [7] and reactive pulsed laser ablation techniques [8].

This work contains the Structural, morphological, and optical properties of Cr_2O_3 thin films deposited by PLD at R.T., and then annealing at 300 °C.

Experimental procedure

PLD technique is used to deposit Cr_2O_3 thin films shows in Fig. 1, where this technique consist of vacuum chamber evacuated to pressure (10^{-2} mbar) and Q-switched Nd: YAG laser. The focused Nd:YAG laser beam at (500-900) mJ comes through a window and incident on surface of the Cr_2O_3 target with an angle of 45°. The substrate is placed in front of target and its surface parallel to it. Suitable gap is kept between substrate and target so that the substrate holder doesn't impede the incident laser beam. The films were deposited on glass at R.T. Q-switched Nd: YAG laser with (1064 nm) wavelength, (pulse width 10 ns) repetition frequency, (10 Hz), for 300 laser pulse used as deposition conditions.

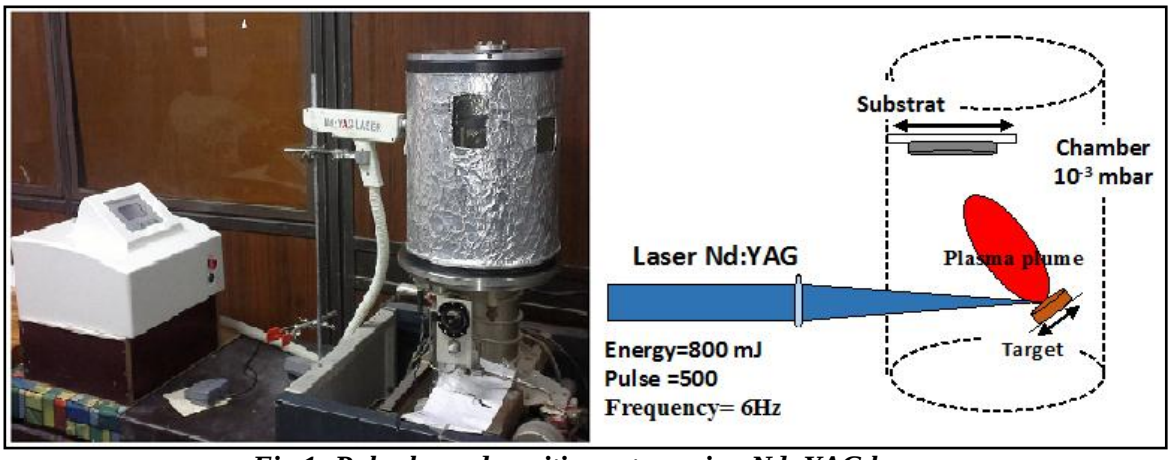

Fig.1: Pulse laser deposition setup using Nd: YAG laser.

Results and discussion

The optical transmittance spectra for Cr_2O_3 thin films prepared by PLD technique at R.T., and annealed at 300 °C; using different energies are shown in Figs. 2 and 3.

It is clear from these figures that for each analyzed thin film it has been noticed that the transmittance decreased with increasing annealing temperature. This is probably due to the improvement in the size of the crystal. It is clear that the annealing temperature has a clear impact on the transmittance decreasing. Transmittance decrease with increase temperature, the Cr_2O_3 films annealed at higher temperatures shows less transmittance values. In the Figs. 2 and 3, the greatest value of transmittance is

in the Near IR range of the spectrum (300-1100) nm almost 99 % at R.T. and 90 % at 300 °C annealing temperature for energy 500 mJ and wavelength equal to 1000 nm. While the lowest value of transmittance is 82 % at R.T. and 74 % for annealed film at energy 900 mJ and wavelength equal to 1000 nm which is well agreed with reported values [9]. Also the optical transmittance depends on the thickness of the film. As the thickness of the thin film increases the transmittance decreases i.e. inverse proportionality between them. It is noted in all Cr_2O_3 films prepared by PLD that optical transmittance value be the highest at high wavelengths. For annealing samples, it is observed that the overall maximum peak shifts towards the shorter wavelength with decrease the energy. This is because in the case of thicker films, more atoms are present in the film so more states will be available for the photons to be absorbed.

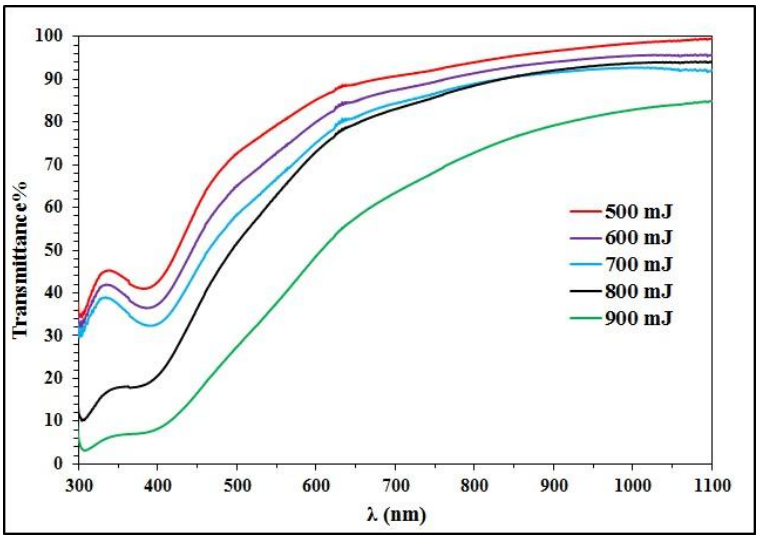

Fig. 2: Transmission versus wavelength of Cr_2O_3 films prepared by PLD at R.T. with different energies.

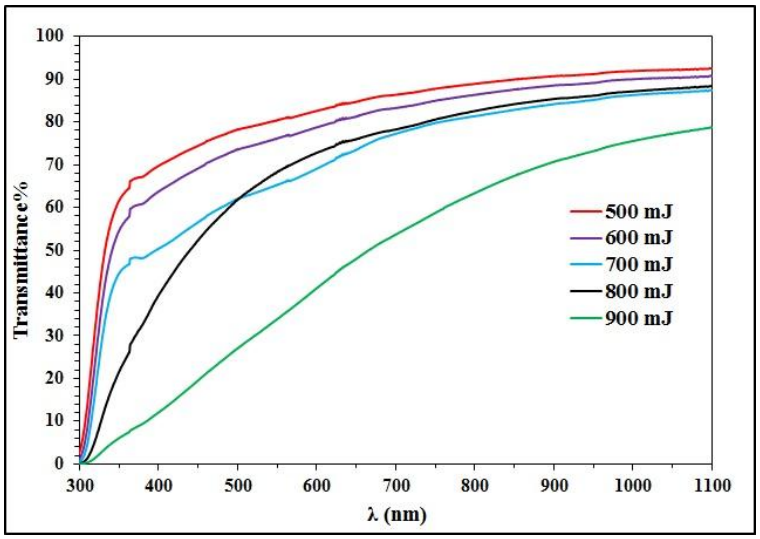

Fig. 3: Transmission versus wavelength of Cr_2O_3 films prepared by PLD at 300 °C annealing temperature with different energies.

We can see from Tables 1 and 2, Figs. 4 and 5, that the absorption coefficient of the Cr_2O_3 films is characterized by strong absorption at

the shorter wavelength region between 300-600 nm at R.T. and 200-350 nm for annealed films. In the shorter wavelength the absorption coefficient exhibits high values of α (α >10^4 cm^{-1}) which means that there is a large probability of the allowed direct transition [10], and then α decreases with increasing of wavelength. Also we can notice from these figures that α increase with increasing of energies of pulse as given in Table 1 and Fig. 4 for samples prepared at R.T. Values of α increase between (0.79–3.22) ×10^4 cm^{-1} with increasing of energies (500-900) mJ at λ= 500 nm wavelength. Same behavior shown in Fig. 5 and Table 2 for samples annealed at 300 °C the values of α increase between (0.60–3.26)×10^4 cm^{-1} with increasing of energies from 500 to 900 mJ.

Table 1: Optical constants of Cr_2O_3 thin films prepared by PLD at R.T., and at λ= 500 nm.

E (mJ)	T%	α (cm^{-1})	k	n	ε_r	ε_i	Eg (eV)	Eg (eV)
500	72.81	7934	0.032	2.640	6.970	0.167	2.7	3.59
600	65.26	10669	0.042	3.038	9.227	0.258	2.65	3.5
700	58.50	13403	0.053	3.410	11.622	0.364	2.6	3.39
800	51.77	16460	0.066	3.791	14.368	0.497	2.5	3.30
900	27.49	32282	0.129	5.004	25.023	1.286	2.35	2.70

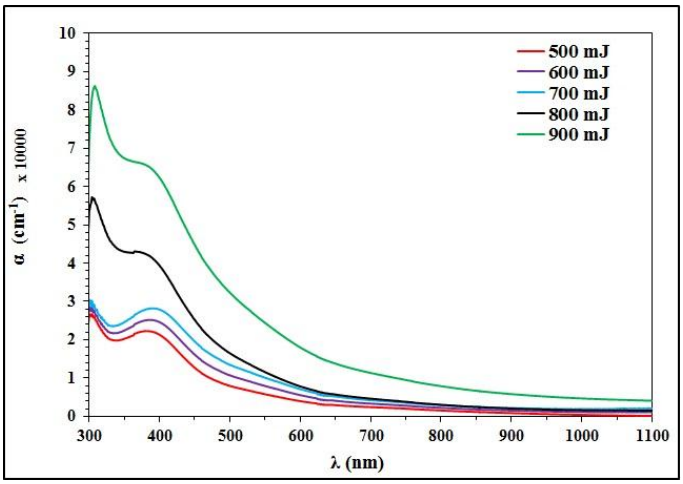

Fig. 4: The absorption coefficient versus wavelength of Cr_2O_3 films coated glass prepared by PLD at R.T. with different energies.

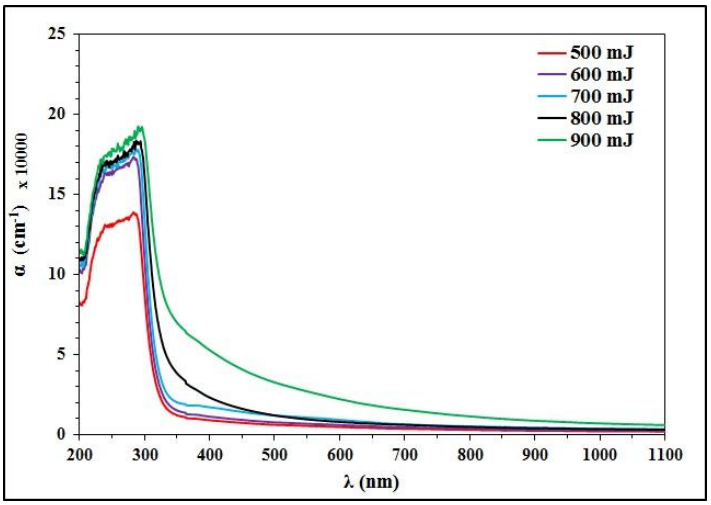

Fig. 5: The absorption coefficients versus wavelength of Cr_2O_3 films prepared by PLD at annealed 300 °C with different energies.

Table 2: Optical constants of Cr_2O_3 thin films prepared by PLD annealed at 300 ^oC, and at λ= 500 nm.

E (mJ)	T%	α (cm^{-1})	k	n	ε_r	ε_i	Eg (eV)
500	78.35	6098	0.024	2.358	5.558	0.114	4.05
600	73.72	7623	0.030	2.593	6.724	0.157	4.02
700	62.11	11907	0.047	3.209	10.298	0.304	3.98
800	61.97	11964	0.048	3.217	10.349	0.306	3.90
900	27.13	32616	0.130	5.014	25.124	1.302	3.80

E_g of Cr_2O_3 thin films prepared by PLD annealed at 300 $^\circ$C larger than E_g of Cr_2O_3 thin films prepared by PLD at R.T., due to increasing the temperature, the energy gap increases because the atoms are re-positioned to the correct locations and energy levels disappears accordingly, then, increasing the energy gap.

Fig. 6 shows he XRD results of Cr_2O_3 films deposited at R.T. by PLD for different energies (500-900) mJ and annealed at 300 $^\circ$C to form phase and achieve the recrystallization process and to get large Cr_2O_3 particles. We deduce that our samples are effectively contains polycrystalline structure. In preference, diffraction peaks at crystalline planes (112), (104), (110), (113), (024), (116) and (300). The peak positions of the Cr_2O_3 planes were observed at 24°, 33.5°, 36°, 41°, 50.5°, 55° and 66°. All the observed peaks are in well agreement with the reported results [11].

All the diffraction peaks in the XRD pattern can be indexed to phase of Cr_2O_3 films deposited by PLD on glass substrates annealed at 300 $^\circ$C, which are in good agreement with the standard values of the reported data (JCPDS no. 38-1479) [12] as the major phase and no secondary phase with a preferred orientation along (104) direction.

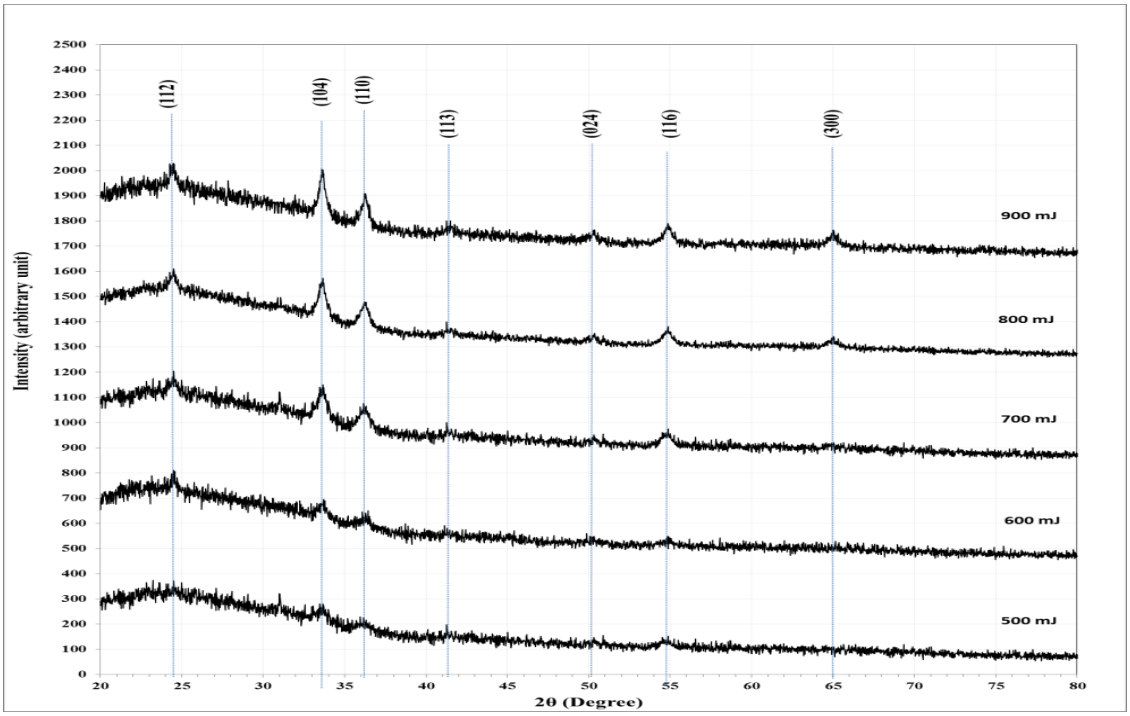

Fig. 6: X-ray diffraction pattern of Cr_2O_3 films prepared by PLD and annealed at 300 ^oC with different energies.

Fig. 7 shows AFM images of the surface topography of Cr_2O_3 thin films. Surface topography parameters and average grain size which were estimated from the granularity copulation distribution are tabulated in Table 3 which is well agreed with reported values [13]. The images of Cr_2O_3 thin film prepared at R.T. shows the surface with uniform island-like topography and some structure of clusters can be clearly observed in figures. These crystallite clusters are the result of crystallites coalescence. The grain sizes of grains in clusters of Cr_2O_3 thin films are in the range of nanometers. In these images, Surface Roughness Average S_a is small which shows very good smoothness of the surface. This means that the prepared films are well deposited.

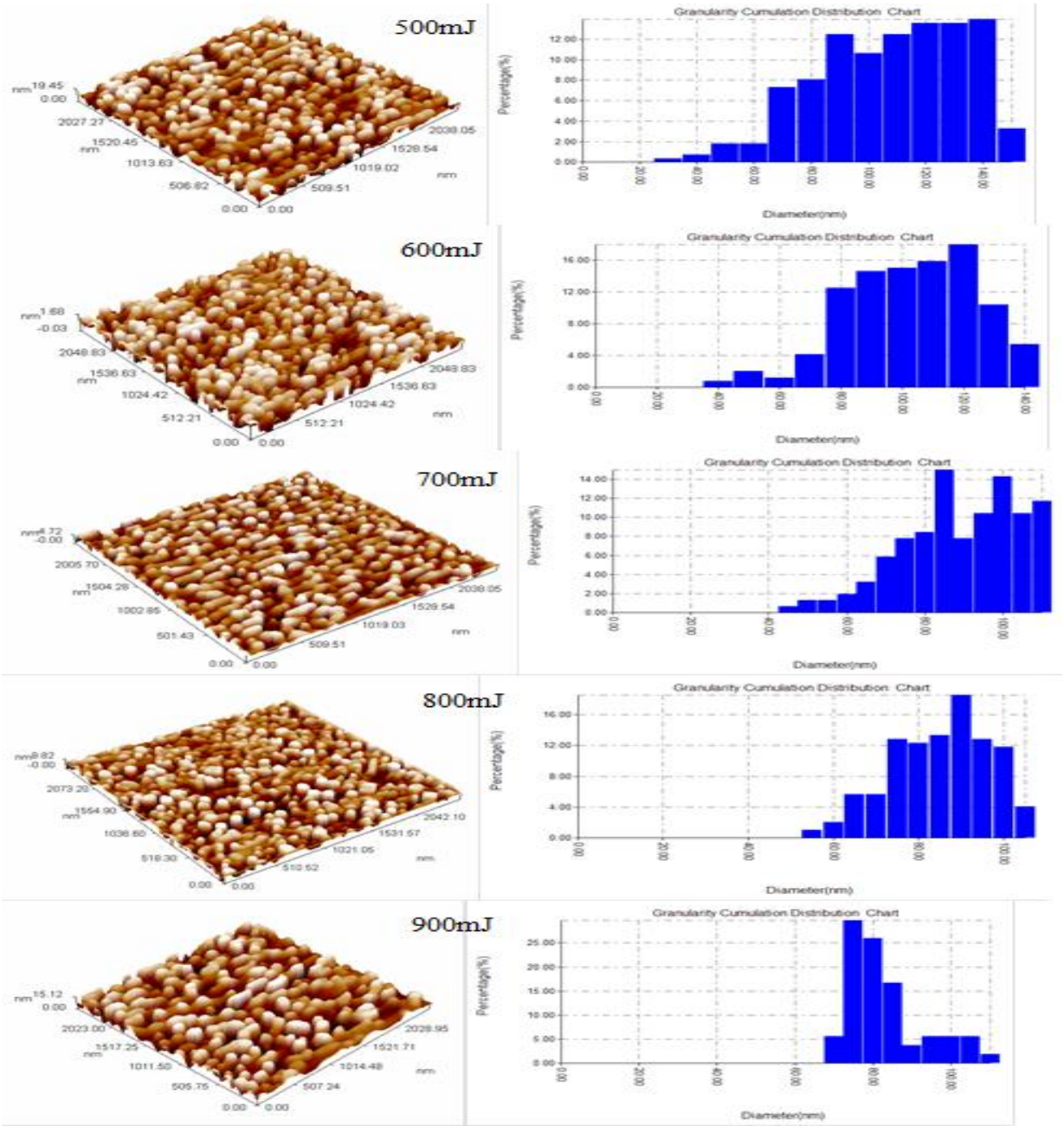

Fig. 7: 3D AFM topography image and distribution chart of Cr_2O_3 film deposited by PLD at R.T. with different energies.

Table 3: Surface topography parameters and grain sizes of Cr_2O_3 thin films.

Energy mJ	Thin film thickness (nm)	Ave. Roughness (nm)	Root Mean Sq. (nm)	Peak To Peak (nm)	Grain size (nm)
500	177.3	4.32	5.9	19.2	80.60
600	199.5	0.375	0.443	1.7	82.64
700	210	1.23	1.22	4.72	86.62
800	249.3	2.19	2.59	9.81	97.92
900	372.4	3.43	4	14.9	102.90

Conclusions

The optical energy gap (E_g) of the Cr_2O_3 films decreases with increasing lasing energy and increased with increased annealing temperature. It is clear that the annealing temperature has a clear impact on the transmittance decreasing; this is a result of increasing the surface roughness of the thin film and increase the scattering of light. Also, the optical transmittance depends on the thickness of the film. The absorption coefficient decreases with increasing of wavelength and increase with increasing of energies.

References

[1] A. M. L. Medeiros, M. A. R. Miranda, A. S. de Menezes, P. M. Jardim, L. R. D. da Silva, S. T. Gouveia, J. M. Sasak, J. Metastable Nanocrystalline Mater., 20–21 (2004) 399-406.

[2] S. Gaelle, Mohamed Kasim, J. Adv. Chem., 10, 1 (2014) 2146-2161.

[3] G. Carta, M. Natali, G. Rossetto, P. Zanella, G. Salmaso, S. Restello, V. Rigato, S. Kaciulis, A. Mezzi, Chem. Vap. Deposition, 11 (2005) 375-380.

[4] X. Pang, K. Gao, F. Luo, H. Yang, L. Qiao, Y. Wang, A. A. Volinsky, Thin Solid Films, 516, 15 (2008) 4685-4689.

[5] T. Maruyama and H. Akagi, J. Electrochem. Soc., 143, 6 (1996) 1955-1958.

[6] S. M. Machaggah, R. T. Kivaisi, and E. M. Lushiku, Sol. Energy Mater.,19, 3–5 (1989) 315-321.

[7] R. H. Misho, W. A. Murad, G. H. Fattahallah, Thin Solid Films, 169, 2 (1989) 235-239.

[8] M. Tabbal, S. Kahwaji, T. C. Christidis, B. Nsouli, K. Zahraman, Thin Solid Films, 515, 4 (2006) 1976-1984.

[9] M. Julkarnain, J. Hossain, K. S. Sharif, K. A. Khan, Canadian Journal on Chemical Engineering & Technology, 3, 4 (2012) 81-85

[10] S. R. Elliott, Physics of amorphous materials, Longman Scientific & Technical, (1984).

[11] Tagreed. M. Al-Saadi, Noor A. Hameed, Advances in Physics Theories and Applications, 44 (2015) 139-148.

[12] F. Farzaneh and M. Najafi, J. Sci. Islam. Repub. Iran, 22, 4 (2011) 329-333.

[13] Ahmed Kadari, Tobias Schemme, Dahane Kadri, Joachim Wollschläger, Results in Physics, 7 (2017) 3124-3129.